

# Mechanical Properties and Fractographical Analysis by Laser Scanning Confocal Microscopy (LSCM) of Laser Textured Bi(Pb)-2212 Superconducting Materials

F. Capel<sup>1,a</sup>, M. A. Madre<sup>2,b</sup>, A. Sotelo<sup>2,c</sup>, M. Mora<sup>2,d</sup>, J. C. Díez<sup>2,e</sup> and J.M. López-Cepero<sup>3,f</sup>

<sup>1</sup> Instituto de Cerámica y Vidrio, C.S.I.C. Campus de Cantoblanco 28049 Madrid (Spain)

<sup>2</sup> Instituto de Ciencia de Materiales de Aragón C.S.I.C.-Universidad de Zaragoza María de Luna, 3. 50018 Zaragoza (Spain)

<sup>3</sup> Departamento de Física de la Materia Condensada, Universidad de Sevilla. Apdo. 1065, 41080 Sevilla (Spain)

<sup>a</sup>[fcapel@icv.csic.es](mailto:fcapel@icv.csic.es), <sup>b</sup>[mmadre@unizar.es](mailto:mmadre@unizar.es), <sup>c</sup>[asotelo@unizar.es](mailto:asotelo@unizar.es),

<sup>d</sup>[mmora@unizar.es](mailto:mmora@unizar.es), <sup>e</sup>[monux@unizar.es](mailto:monux@unizar.es), <sup>f</sup>[cepe@us.es](mailto:cepe@us.es)

**Keywords:** Bi-2212, zone melting, mechanical strength, confocal microscopy, Weibull parameters.

## Abstract

Vitreous cylinders with compositions  $\text{Bi}_{2-x}\text{Pb}_x\text{Sr}_2\text{CaCu}_2\text{O}_y$ , ( $x = 0$  and  $0.4$ ) were prepared and used as precursors to fabricate textured bars through a Laser Floating Zone melting method (LFZ). The resulting textured cylindrical bars were annealed and were mechanically characterized through mechanical strength,  $\sigma$ , Young modulus,  $E$ , Vickers hardness,  $H$ , and Weibull parameters,  $S_0$  and  $m$ . The study of the mechanisms controlling the fracture process was made by means of the fractographical analysis using Laser Scanning Confocal Microscopy (LSCM). Finally, the microstructure was determined and correlated with the mechanical properties.

## INTRODUCTION

One of the most attractive applications of  $\text{Bi}_2\text{Sr}_2\text{CaCu}_2\text{O}_{8+\delta}$  (Bi-2212) superconductors is their use in fault current limiters [1], providing the possibility to develop resistive-type fault current limiters. These would require the fabrication of Bi-2212 materials capable of supporting high critical current densities in the superconducting state and developing high resistance in the normal state, to effectively limit the fault current. However, the successful use of Bi-2212 superconducting ceramic materials as current limiters is conditioned by the low slope of the V-I curves that are obtained in the transition from the normal to the superconducting state. One solution to overcome this problem is based on the use of long length samples. Another alternative way is the cationic substitution, which could introduce effective flux pinning centers and increase the slope of the V-I curves. In particular, the partial Bi substitution with Pb has shown to be useful to increase the intragranular pinning properties in single crystals, leading to the enhancement of both irreversibility field and critical current density [2, 3]. On the other hand, it has been shown that LFZ samples with a nominal composition  $\text{Bi}_{1.6}\text{Pb}_{0.4}\text{Sr}_2\text{CaCu}_2\text{O}_{8+\delta}$ , exhibit higher slope in the superconducting to normal transition than the undoped ones [4].

In this context, therefore, it is important to know how the Pb addition affects the mechanical properties of the LFZ Bi-2212 materials. For this study, a melt quenching method has been applied to obtain long precursor bars (more than 20 cm) by quenching the molten material inside silica tubes of 2 mm inner diameter. In order to texture these materials, a Laser Floating Zone Melting (LFZ) technique has been used [5]. In this work, the changes on the mechanical properties in LFZ textured materials has been studied and related to the Pb addition.

Materials so obtained were mechanically characterized through mechanical strength,  $\sigma$ , Young modulus, E, Vickers hardness, Hv and Weibull parameters. Finally, the study of the mechanisms controlling the fracture process was made by means of the fractographical analysis, using laser scanning confocal microscopy (LSCM) [6]. LSCM is an optical microscopy technique whose main distinctive

feature is a very narrow diaphragm (a pinhole) that discards out of focus light. Thus, a LSCM image consists only of light from a thin, well-defined focal plane, being a "virtual section" of the sample at the height of the focal plane. If a number of sections with varying focal plane positions are acquired, a height map of the sample can be calculated and used to build 3D views and height profiles of the surface.

## EXPERIMENTAL

$\text{Bi}_{2-x}\text{Pb}_x\text{Sr}_2\text{CaCu}_2\text{O}_{8+\delta}$ , with  $x = 0$ , and  $0.4$  have been prepared from commercial  $\text{Bi}_2\text{O}_3$  (Panreac, 98+%),  $\text{PbO}$  (Panreac, 99+%),  $\text{SrCO}_3$  (Panreac, 98+%),  $\text{CaCO}_3$  (Panreac, 98.5+%) and  $\text{CuO}$  (Panreac, 97+%) powders. They were weighted in the adequate atomic proportions, mixed in a ball mill and thermal treated twice under air (12h at 750 and 780 °C) to decompose the carbonates and decrease the volume of the mixture (about 50% in the first step and 35% in the second). This prerreacted mixture was then introduced into a Pt crucible and melted at 1050-1075 °C to assure good homogeneity and fluidity of the liquid. The obtained melt was then quenched into silica tubes, 2 mm inner diameter, to obtain long (up to 25 cm) and homogeneous cylindrical bars [7].

The obtained cylinders were processed with a LFZ technique. In this process, the precursor bars are melted by the incidence of a Nd:YAG laser (1064 nm) under air. This melt is directionally solidified, at a growth rate of 40 mm/h on a seed of the same material, obtaining a highly oriented microstructure. This processing procedure is described in detail elsewhere [5]. In order to obtain the appropriate phase composition (Bi,Pb-2212), the as grown samples were annealed at 835 °C 60 h, followed by 12 h at 800 °C and quenched to room temperature.

The mechanical strength was performed on a four-point bending apparatus. The tests were made at a loading rate of 0.5 mm/min. To determine Young modulus, the deflection measurements in flexural strength test were used. The microhardness was determined by means of indentation tests. For testing purposes, samples were dipped into a resin and then polished until bright. In order to carry out the hardness measurements, a Vickers indenter and a Leco

microhardness tester were used. Loads of 9.8 N were applied for 15 s. From the patterns, i.e. from the measurements of the indentation semi-diagonals, the hardness values were computed.

To characterize the fracture of the two samples, the failure strength data were analyzed using the known Weibull approach [8]. If the failure of the samples is assumed to be surface flaw controlled, the probability of failure,  $\phi$ , of the samples containing a statistical distribution of non-interacting flaws is given by

$$1-\phi = \exp [-(\sigma/S_0)^m] \quad (1)$$

where  $S_0$  and  $m$  are the scale and the shape parameters, respectively. Taking the logarithm twice, equation 1 can be written as

$$\text{Ln Ln } [1/(1-\phi)] = m \text{ Ln } \sigma - m \text{ Ln } S_0 \quad (2)$$

This is a linear equation with slope  $m$ . The expected value of  $\phi$  is obtained from the ordered data where  $\phi = i/(n+1)$ , in which  $i$  is the  $i^{\text{th}}$  order of failure and  $n$  is the total number of specimens in the test.

For the LSCM study, a Leica TCS-SP2 confocal microscope was used. The images were acquired in reflection mode, with a blue Ar laser (488 nm) as the light source. The objectives used were 10x air (for the global views) and 20x air (for the detail views), which have 1.5 mm and 750  $\mu\text{m}$ , respectively, as maximum lateral field of view. Typically, about 250 images were acquired for each heightmap, with 1-2  $\mu\text{m}$  height steps.

## RESULTS AND DISCUSSION

Analysis of the vitreous precursor materials through SEM micrographs and EDX mapping show that the starting material is very homogeneous along the bars. After texturing, a highly orientated microstructure is obtained, as can be seen in Fig. 1. In the as grown samples, the texture can be reflected through the dark phases orientation. Three main phases and contrasts can be found on the micrographs: dark gray contrast phase, related to Bi-free secondary phases; gray contrast, related to Bi-2201/Bi-2212 intergrowths; and light gray contrast, related to Bi-2201. Also, a minority phase associated to secondary phases rich in Ca and free of Bi, black contrast, can be observed in Fig. 1 (c and d), smaller in size than the

previously described ones. The main difference among the samples with and without Pb is the increase in the amount of secondary phases (dark gray contrast) and the misorientation of the Bi-rich phases (gray and light gray contrasts) when Pb is added.

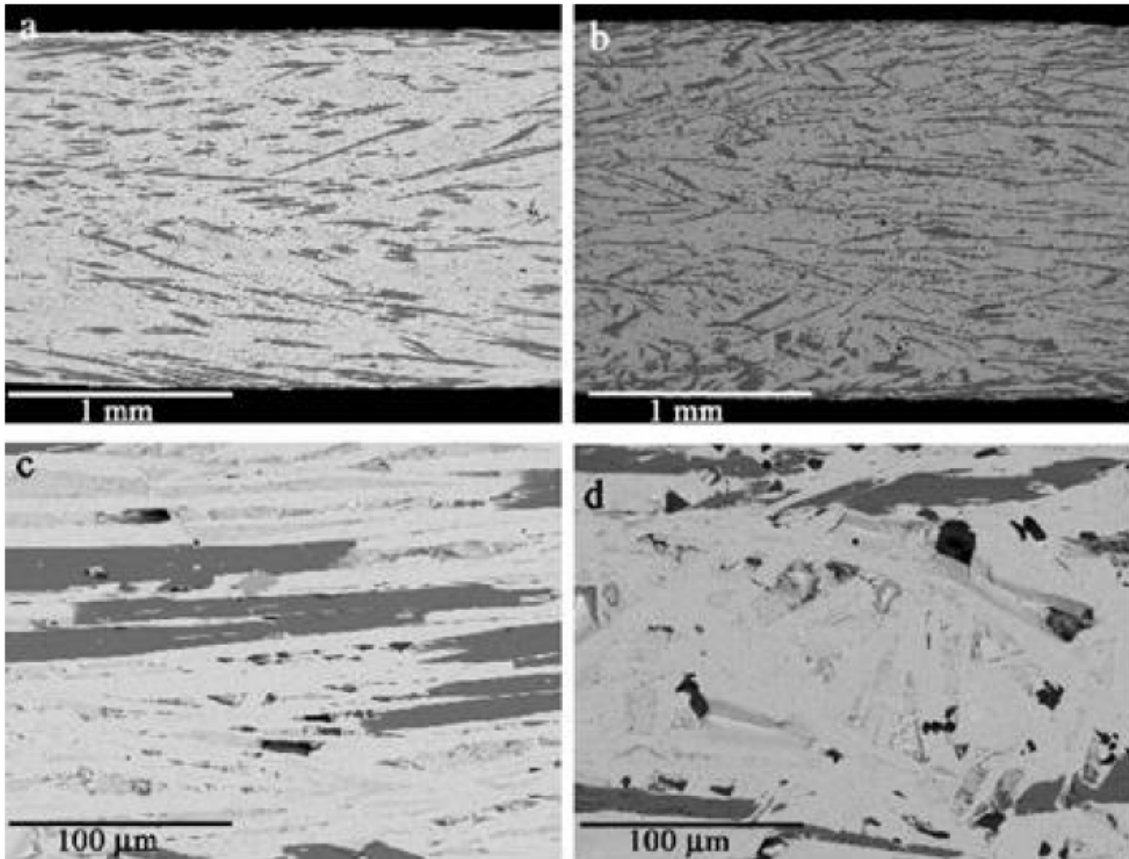


**Fig. 1** Longitudinal SEM micrographs, showing a general view of the as grown samples for  $x = 0$  (a) and  $0.4$  (b) and detail of the centre of the as grown samples for  $x = 0$  (c), and  $0.4$  (d). Bi-free phases are shown as dark contrast.

After annealing, the undoped samples show a more homogeneous microstructure and smaller amount of secondary phases, which are concentrated on the outer zone of the cylinders. In contrast, the doped samples have a bigger amount of secondary phases on the entire sample, as can be seen on Fig. 2. In all the samples, resistivity measurements have shown that the Bi-2212 phase is developed. On the doped samples, Pb is found not only in the superconducting phase, but also in plumbate-like phases. The difference on the microstructure has great influence on the mechanical properties of the samples.

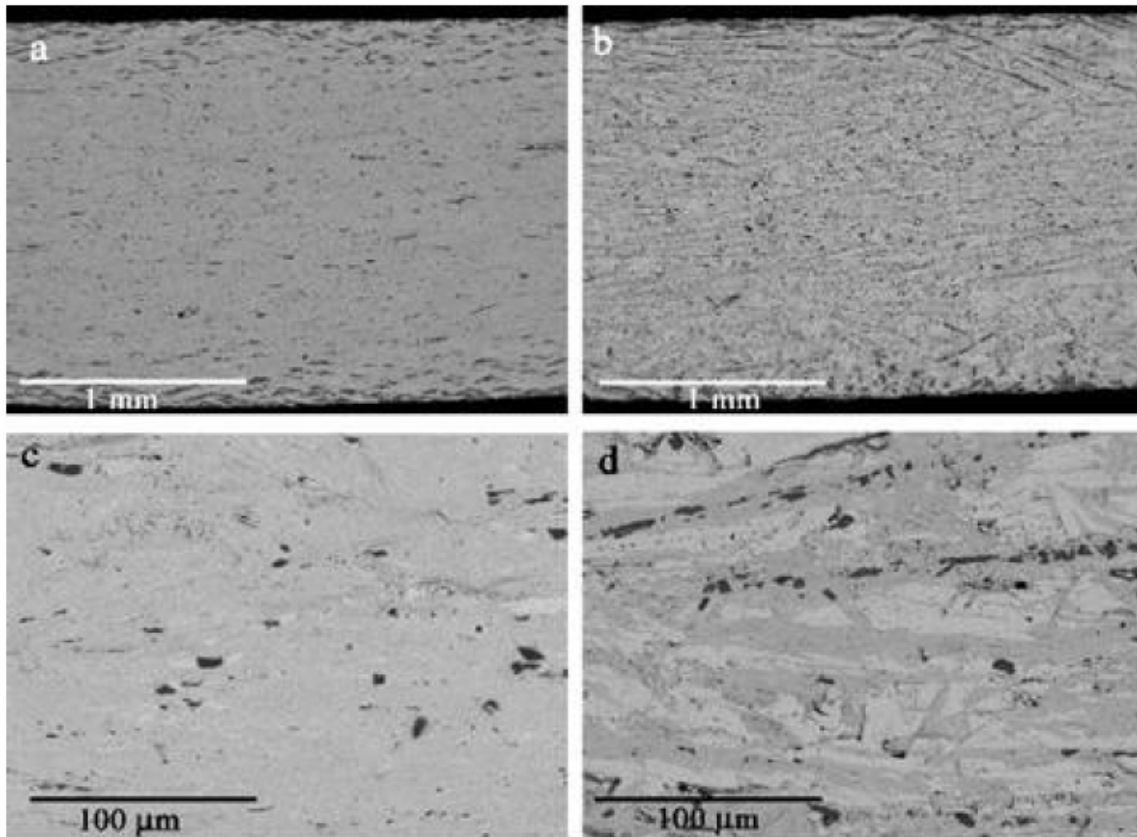


**Fig. 2** Longitudinal SEM micrographs, showing a general view of the annealed samples for  $x = 0$  (a) and 0.4 (b), and detail of the centre of the annealed samples for  $x = 0$  (c) and 0.4 (d).

Table I gives the results obtained for  $\sigma$ ,  $E$ ,  $H_v$  and Weibull parameters. As can be seen from this table, the hardness of the Pd doped samples is higher than the undoped ones due to, probably, the presence of bigger amount of secondary phases. In both samples hardness measurements reveal that radial cracks were not formed during unloading (Fig. 3). In undoped samples the values obtained of  $\sigma$  and  $E$ , are higher than the ones exhibited by the Pb doped. However, there is a greater dispersion in these values, as it is demonstrated by Weibull shape parameter.

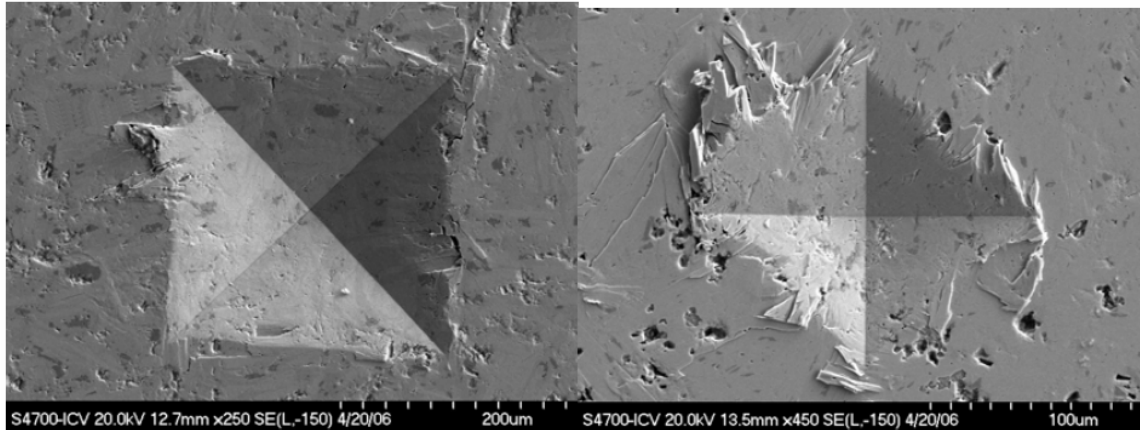


**Fig. 3** Vickers indentation morphologies showing the complete absence of cracking during the unloading: a) doped, and b) undoped samples.

**Table I** Measured mechanical properties on doped and undoped samples.

SAMPLE	Hv (MPa)	$\sigma_f$ (MPa)	E (GPa)	Weibull parameters	
				So	m
0.4 Pb Doped	295±10	156±10	75±5	164	18,2
Undoped	205±10	165±30	85±15	175	7,2

To illustrate the fracture characteristics of the samples, two representative examples, one doped and another undoped, have been studied with LSCM. For each sample, two height maps (a global one and a detail), as well as 3D views and profiles of these height maps, have been acquired and calculated. The undoped sample fracture surface may be observed in Fig. 4a. Qualitatively, it has two main characteristics to remark. First, the visible "hill" at the center-right has very abrupt height changes, giving the sample a stairway-like appearance, with sharp "steps" separated by plateau-like regions with comparatively small roughness. The greater height difference is about 400  $\mu\text{m}$  as obtained from the profiles of the height maps. Second, the whole surface of the sample has a texture which could be described as "fibrous", with prominent linear features; these features also show the step-plateau behaviour of the main hill, albeit in a less pronounced way.

When comparing the fracture surface of the Pb doped (Fig. 4.b) with the undoped samples, some differences are easily noticeable. Firstly, the fracture surface shows a rougher look and is flatter than undoped one. The greater height difference in this case is about 250  $\mu\text{m}$ . Secondly, the linear structures, that gave the undoped

sample its fibrous appearance, are less pronounced, more irregular and their distribution is more random.

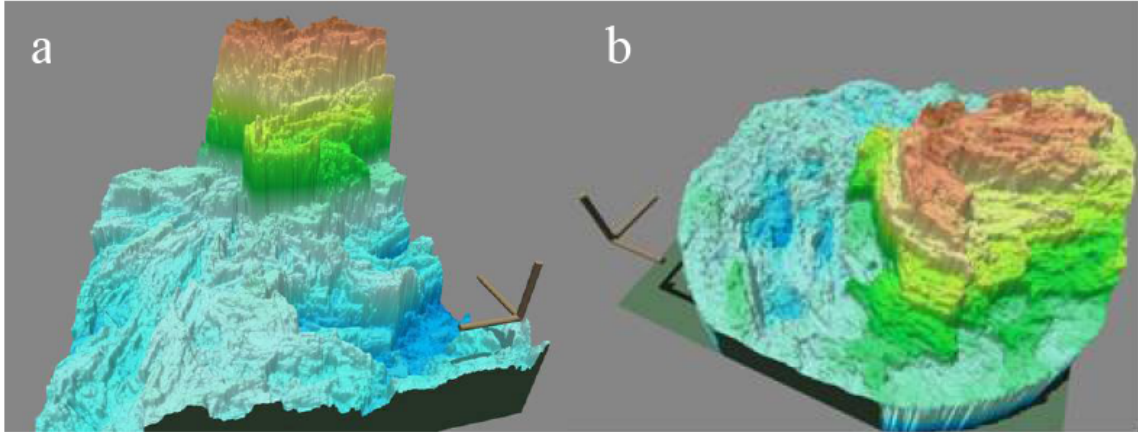


**Fig.4** Fracture surface of the undoped (a) and Pb doped sample (b) obtained from LSCM.

It is very clear that there is an underlying feature common to both samples, namely the "fibrous" texture. In the undoped case this texture is clearly defined, present throughout the whole surface, and is accompanied by abrupt height steps which give the surface a stair-like appearance. The dramatic steps in height are indicative of the accumulation of a high amount of elastic energy just before fracture. In the Pb doped sample, however, the surface does not present abrupt height changes and the base texture is not as extended or well defined. These results, consequently, are in agreement with the microstructure of the doped and undoped samples shown in fig. 2 and 3, and clearly justify the mechanical behaviour of the analyzed samples.

## CONCLUSIONS

Some of the most important conclusions of this article are reiterated below:

It has been found an anomalous brittle fracture of the (Bi-2212) and Bi-Pb 2212 superconductors, showing no cracks after on the edges of the indentation. SEM and LSCM microscopy agree with the mechanical properties measurements, showing that lead addition eases fracture initiation and propagation, yielding fracture surfaces with less marked features and a flatter overall shape, leading to a decrease of  $\sigma$  and E.



## References

- [1] W. Paul, *et al.* Physica C 354 (2001), p 27
- [2] I. Chong, *et al.* Science Vol. 276, (1997), p 770
- [3] N. Musolino, *et al.* Physica C 399, (2003), p 1
- [4] A. Sotelo, *et al.* Bol. Soc. Esp. Ceram. V. (*in press*)
- [5] G. F. de la Fuente, *et al.* Adv. Mater. 7, (1995), p 853.
- [6] J. M. López-Cepero, *et al.* Key Eng. Mater 290 (2005) p 280
- [7] A. Sotelo, *et al.* Proceedings of VIII Congreso Nacional de Materiales. (2004). ISBN: 84-9705-594-2, S PUPV (CL).
- [8] W. Weibull. J. Appl.Mech. 1951, 293